Communications in Nonlinear Science and Numerical Simulation 121 (2023) 107204

Contents lists available at ScienceDirect

Communications in Nonlinear Science and Numerical Simulation

journal homepage: www.elsevier.com/locate/cnsns

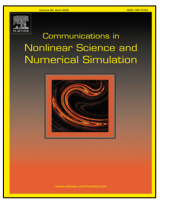

Research paper

Nonlinearity of the volume–volatility correlation filtered through the pointwise Hurst–Hölder regularity

Massimiliano Frezza [a], Sergio Bianchi [a,b,*], Augusto Pianese [c]

[a] MEMOTEF, "Sapienza" University of Rome, Rome, Italy
[b] Intl Affiliate, Dept. Finance and Risk Engineering, New York University, NY, USA
[c] QuantLab, University of Cassino and Southern Lazio, Italy

ARTICLE INFO

Article history:
Received 31 October 2022
Received in revised form 1 February 2023
Accepted 2 March 2023
Available online 6 March 2023

Keywords:
Volume–volatility relationship
Efficient Market Hypothesis
Martingale model
Hurst–Hölder exponent

ABSTRACT

We identify market inefficiency as a pivotal explanatory variable of the puzzling volume–volatility relationship. The result, that can bring together into a coherent framework many apparently conflicting findings, follows from translating the realized volatility into the corresponding pointwise Hurst–Hölder exponent. This allows to measure, at any time t, markets' departures from the martingale property, i.e. from efficiency as stated by the Efficient Market Hypothesis. We find that when efficiency is not accounted for, a positive contemporaneous relationship emerges; conversely, it disappears as soon as efficiency is taken into account.

1. Introduction

An extensive literature document a positive relation between price volatility and trading volume in the financial markets, but the causal connection originating such a relation represents an open and challenging question, from both a theoretical and empirical point of view. Various models, which can be regarded as complementary rather than competitive [1], have been introduced to explain this relationship. They include the long debated *Mixture of Distributions Hypothesis* (MDH) [2–8]; the *Sequential Arrival of Information Hypothesis* (SAIH) [9–13]; the *Dispersion of Beliefs Hypothesis* (DBH) [14–17]; the *Noise Trader Hypothesis* (NTH) [1,18,19].

The MDH posits that both volume and volatility are driven by the same underlying information flow, i.e. both change simultaneously as soon as information is processed by market participants. As a consequence, the volatility per transaction is monotonically related to the volume of the same transaction. The basic version of the MDH does not consider effects as the lagged reactions to news or the interaction among types of traders. This simplification is questioned by the SAIH, which aims to explain the evidence of a lead–lag relationship between returns and volumes. The DBH, which can coexist with both the MDH and the SAIH, posits that a greater dispersion in traders' beliefs generates excess volatility and volume. Since informed traders generally share homogeneous beliefs about fair prices, they tend to trade within a small range of prices around the fair value. By contrast, uninformed traders have more heterogeneous beliefs because they do not properly assess their relative positioning with respect to the fair value; as a consequence, they are less capable to interpret the noisy signals from volume and price changes, what causes excess volatility and volume. Similarly, the NTH focuses on how the activity of uninformed noise traders can destabilize the information proxied by excess trading volume, potentially creating mispricing and causing informed (institutional) traders to respond to the noisy trading rather than to fundamentals.

* Corresponding author at: MEMOTEF, "Sapienza" University of Rome, Rome, Italy.
E-mail address: sergio.bianchi@uniroma1.it (S. Bianchi).

https://doi.org/10.1016/j.cnsns.2023.107204
1007-5704/

Even if it is still unclear when each of the above mechanisms prevails on the others, it is almost obvious that the number of investors participating in the market can enhance liquidity provision and mitigate volatility. However, both the lack and the excess of liquidity entail market inefficiency: while the former typically characterizes the stock market crashes, the latter can lead to bullish mispricing and speculative bubbles. In both cases, pathological patterns appear that ultimately imply a deviation of the market from its physiological condition of efficiency. In this regard, a large number of contributions document that efficiency actually is nothing but the result of imbalances that can last even for relatively long spans of time [20–25]. This suggests that a deeper understanding of the volume–volatility relation can come from analyses conditional to the level of efficiency of the market. Thus, the idea behind our contribution is to investigate the volume–volatility relationship by distinguishing between volatility that is "too low" or "too high" relative to values compatible with market efficiency.

Several approaches have been studied to account for and tackle inefficiencies in financial markets. For example, using the local entropy and the symbolic time series analysis, Risso [26] measures the evolution of the daily informational efficiency for different stock market indices and finds some evidence that the probability of having a crash increases as the informational efficiency decreases. A similar approach is proposed in a recent contribution by Brouty and Garcin [27]; using the Shannon entropy applied to a symbolic representation of price returns at a given time scale, they construct an indicator of the information embedded in the data and derive its exact and asymptotic distribution when the Efficient Market Hypothesis holds, developing a statistical test of market efficiency. In Ito et al. [28] a non-Bayesian time-varying vector autoregressive model is developed to estimate the time-varying market efficiency in G7 countries. Very recently, considering an alpha-stable distribution and a dependence structure between price returns, Ammy-Driss and Garcin [29] provide a dynamic estimation method for the Hurst exponent and the memory parameter of a fractional Lévy-stable motion, two efficiency indicators. Examining the effects of COVID-19 pandemic, they find strong inefficiencies for US indices as compared to Asian and Australian indices. Other approaches combine several indicators to study the phenomenon: e.g. Feng et al. [30] use the correlation-corrected balanced estimation of diffusion entropy to evaluate the evolution of the local scaling behavior of exchange rate series, and find that during the global financial crisis the scaling behavior displays distinctive patterns; Kristoufek and Vosvrda [31] introduce a measure of efficiency based on the correlation structure of the returns and the local herding behavior revealed by a low fractal dimension. Applying their measure to a portfolio made of 41 stock indices, they discriminate different degrees of efficiency among markets referred to different geographic areas.

All these contributions, whose list is obviously far from being exhaustive, suggest that it is reasonable assuming that market (in)efficiency is related somehow to the degree of regularity of stock prices. Starting from this posit, we model the stock market by means of a general and flexible class of stochastic processes precisely built to let the degree of regularity change through time. We refer to "a class" of stochastic processes because – as detailed in Section 2 – many models share the property of a time-changing regularity. Mostly, such models have in common the fact that they locally behave as a fractional Brownian motion, in the sense that their local regularity at time t_0 (measured by the local Hurst–Hölder exponent in a neighborhood of t_0) equals the exponent of a fractional Brownian motion of parameter $H(t_0)$. Assuming that the stock price owns this property, we introduce and theoretically justify the Hurst–Hölder dynamical exponent as a measure of market efficiency. Following this approach, we bring to light nonlinearities that are not detected when analyzing the relationship as a whole. In fact, if volumes and volatility provide informative support about the current market sentiment, their explanatory power finds its fulfillment when combined with other variables such as, for example, market efficiency imbalances. Market phases depicted by a strong positive relationship between volumes and price regularity may reveal inefficiencies, which can be thought as a sort of perturbed elastic force applied to an equilibrium state. The stronger the impact of new information the stronger the force, with arbitrage opportunities acting as a damping friction which tend to restore the equilibrium condition. This mechanism clearly provides insights for both traders and regulators: the former could exploit it to decide the timing of their buy/sell orders; the latter could assess more easily and timelier where and when inefficiencies arise.

The remainder of the paper is organized as follows: in Section 2 we motivate why the local degree of market efficiency can be captured by the Hurst exponent; in Section 3, using a class of estimators based on variation statistics, an explicit relationship is established between volatility and Hurst–Hölder exponent; finally, in Section 4 we analyze the conditional nonlinearities appearing in the volume–volatility relation for the index S&P500.

2. Market efficiency through the Hurst–Hölder exponent

We preface the definitions of pointwise and uniform Hölder exponent, which quantify the (Hölder) regularity of the paths of a stochastic process and will be useful in the sequel.

Let $(X_{t,\omega} : t \in T, \omega \in \Omega)$ be a random field with continuous and nowhere differentiable trajectories, defined over a rectangle $T \subset \mathbb{R}^d$.

Definition 1. *The pointwise Hölder exponent of* $(X_{t,\omega})$ *in a neighborhood of point* t *is the stochastic process* $(\alpha^X_{t,\omega} : t \in T)$ *defined as*

$$\alpha^X_{t,\omega} := \sup\left\{\alpha : \limsup_{h\to 0} \frac{|X_{t+h,\omega} - X_{t,\omega}|}{|h|^\alpha} = 0\right\}$$

$(\alpha^X_{t,\omega} : t \in T)$ *measures the local Hölder regularity of* $(X_{t,\omega})$ *at* t.

When $(X_{t,\omega})$ is a continuous Gaussian process, by virtue of zero–one law, there exist a non random quantity a_t^X such that $\mathbb{P}(\alpha_{t,\omega}^X = a_t^X) = 1$.

Definition 2. *Let $J \subset T$ be a non-degenerate rectangle. The uniform Hölder exponent is the stochastic process*

$$\beta_{J,\omega}^X := \sup\left\{\beta : \sup_{s,s' \in J} \frac{|X_{s,\omega} - X_{s',\omega}|}{|s - s'|^\beta} < \infty\right\}.$$

$\beta_{J,\omega}^X$ measures the global Hölder regularity of $(X_{t,\omega})$ over J.

It is $\beta_{J,\omega}^X \le \inf_{t\in J} \alpha_{t,\omega}^X$.

The Efficient Market Hypothesis [32] posits that a market is efficient if the discounted price sequence (S_t) reflects information $\mathcal{F}_t$ accumulated up to time t. The condition translates into requiring that (S_t) be a martingale. The Lévy's characterization theorem states that the continuous stochastic process $(B_t, t \ge 0)$, adapted to a right-continuous filtration $(\mathcal{F}_t, t \ge 0)$, is an $\mathcal{F}_t$-Brownian motion if and only if B is a local martingale and its quadratic variation $\langle B\rangle_{2,t} = t$.

Starting from '80s, the many controversial results about the Brownian nature of the price sequences (see e.g. [33] for a review) led to consider alternative models such as the fractional Brownian motion (fBm) with Hurst parameter $H \in (0, 1)$ [34]. Defined as the only zero mean, self-similar Gaussian process with covariance

$$\mathbb{E}(B_t^H B_s^H) = \frac{1}{2}(t^{2H} + s^{2H} - |t - s|^{2H}), \tag{2.1}$$

the fBm has (i) Hölder continuous paths of order α, for any $\alpha \in (0, H)$, (ii) $\frac{1}{H}$-variation on any time interval $[0, t]$ equal to $\mathbb{E}(|B_1^H|^{1/H})t$ [35,36]; (iii) pointwise and uniform Hölder exponents almost surely equal to the Hurst exponent H [37,38]. Thus, the Hurst parameter dictates the regularity of the paths of the fBm: for $H \in (0, 1/2)$, the trajectories are rougher and rougher as the distance $1/2 - H$ increases; in contrast, for $H \in (1/2, 1)$, the trajectories are smoother and smoother as the distance $H - 1/2$ increases.

From the Lévy's characterization theorem and condition (ii) it follows that the fBm is not a semimartingale except when $H = 1/2$, case in which it reduces to a Brownian motion. Furthermore, conditions (i)-(iii) allow to characterize the martingale property through the value of the Hurst–Hölder exponent, provided that one refers to the class of processes that locally behave as the fBm.[1]

Since for modeling purposes a constant H can be too limiting, the fBm is further generalized into the multifractional Brownian motion (mBm) [37], defined replacing H by an $\eta \in (0, 1)$-hölderian function H_t aimed to ensure the square integrability of the process. Even more recently, Loboda et al. [40] and Ayache and Bouly [41] study an mBm with random Hurst exponent, which they refer to as Itô-mBm and show that the process is locally self-similar in the sense stated below (see Eq. (2.3)). The mBm $B_t^{H_t}$ has covariance function

$$\mathbb{E}(B_t^{H_t} B_s^{H_s}) = D_{H_t,H_s}\left(|t|^{H_t+H_s} + |s|^{H_t+H_s} - |t - s|^{H_t+H_s}\right). \tag{2.2}$$

where $D_{H_t,H_s} = \frac{\sqrt{\Gamma(2H_t+1)\sin(\pi H_t)\Gamma(2H_s+1)\sin(\pi H_s)}}{2\Gamma(H_t+H_s+1)\sin\left(\frac{(H_t+H_s)\pi}{2}\right)}$ is a normalizing factor which ensures unit variance at unit time. If $\beta_{[0,1],\omega}^H > \sup_{t\in[0,1]} H_t$ then, for any non degenerate $J \subset [0, 1]$, $\alpha_{t,\omega}^{B^{H_t}} \overset{a.s.}{=} H_t$ and $\beta_{J,\omega}^{B^{H_t}} \overset{a.s.}{=} \inf_{t\in J} H_t$, that is, with probability 1, the pointwise Hölder exponent of the mBm equals H_t and the uniform Hölder exponent of the mBm over J equals $\inf_{t\in J} H_t$ [37,42].

Unlike fBm, the increments of mBm are no longer stationary, but Benassi et al. [43] prove that if $\sup_t H_t < \min(1, \eta)$, at any point t there exists an fBm with parameter H_t tangent to the mBm (see [44] for a discussion of tangent processes). In other words, the mBm locally behaves like an fBm in the sense that, at any point t

$$\lim_{\epsilon\to 0^+}\left(\frac{B_{t+\epsilon u}^{H_t} - B_t^{H_t}}{\epsilon^{H_t}}\right)_{u\in\mathbb{R}^+} \overset{d}{=} C^{\frac{1}{2}}\left(B_u^{H_t}\right)_{u\in\mathbb{R}^+}. \tag{2.3}$$

where $\overset{d}{=}$ denotes the equality in distribution and $C^{1/2}$ is a scale parameter which ensures that the mBm has variance C at unit time [45]. Relation (2.3) justifies the estimation of H_t by using quadratic variation estimators originally introduced to estimate the constant parameter H of an fBm (see Section 3).

Under the assumption of a market whose prices can be modeled by a process that locally behaves as an fBm, properties above suggest that H_t is much more informative than volatility, because it accounts for both irregularity and departure

[1] This class is somewhat extensive, since it includes not only the multifractional Brownian motion (mBm) and the Multifractional Processes with Random Exponents (MPRE), recalled in the following as natural generalizations of the fBm, but also the Generalized multifractional Brownian motion (GmBm), the bifractional Brownian motion and the mixed fBm, the Weyl and Riemann–Liouville fractional Ornstein–Uhlenbeck (fOU), the fractional Riesz–Bessel motion (fRBm), or the Generalized Cauchy Process (GCP) (see [39] for a review). The characterization does not necessarily hold if, e.g., time-changed processes are introduced. In fact, while the martingale property is preserved by continuous time change, the Hölder property is generally not.

Table 1
Financial interpretation of H_t.

H_t	Stochastic properties	Agents' beliefs	Market pattern
$>\frac{1}{2}$	Persistence Smooth paths $\langle X\rangle_{2,t}=0$	New information confirm outstanding positions	"*Low*" volatility - Momentum Positive inefficiency (PI) Overconfidence/Underreaction
$=\frac{1}{2}$	Independence Martingale $\langle X\rangle_{2,t}=2$	Information fully incorporated by prices	"*Normal*" volatility Sideways market Efficiency (E)
$<\frac{1}{2}$	Mean-reversion Rough paths $\langle X\rangle_{2,t}=\infty$	New information disrupt outstanding positions	"*High*" volatility - Reversals Negative inefficiency (NI) Overreaction

from the martingale case. Furthermore, unlike volatility (whose value can be judged "high" or "low" only by comparison with the previous ones), H_t is an absolute and not a relative indicator. These arguments along with the existence of a relationship that we document in Section 3 between the pointwise Hölder exponent at t and the volatility at the same time, motivated us to study the volume–volatility relationship in terms volume-Hurst/Hölder exponent relationship, according to the financial interpretation given Table 1 [46,47].

3. Estimation of H_t

Variation statistics have been extensively used to estimate the pointwise Hurst–Hölder exponent of a real financial time series. Detailed discussions, to which we refer, can be found in [48–51]. In the following, we will recall only some steps to clarify the relationship that links the volatility to the Hurst–Hölder exponent.

Following [24,52], we consider n observations of mBm X equally spaced with respect to the unit time interval [0, 1]. By virtue of limit (2.3), one has

$$X_t - X_{t-\frac{1}{n}} \sim \mathcal{N}\left(0, C\left(\frac{1}{n-1}\right)^{2H_t}\right) \tag{3.1}$$

for $t = \frac{2}{n}, \dots, 1$. Since the kth absolute moment of a normal r.v. $Y \sim \mathcal{N}(0,\sigma^2)$ equals $\mathbb{E}\left(|Y|^k\right) = \frac{2^{k/2}\Gamma((k+1)/2)}{\Gamma(1/2)}\sigma^k$, introducing a window of size $\nu \ll n$ (with ν even) and considering $t > \frac{\nu}{n}$, the quantity

$$M_t^{(k)} = \frac{1}{\nu}\sum_{i=0}^{\nu-1} |X_{t-\frac{i}{n}} - X_{t-\frac{i+1}{n}}|^k \tag{3.2}$$

satisfies

$$\mathbb{E}\left(M_t^{(k)}\right) = \frac{2^{k/2}\Gamma((k+1)/2)}{\Gamma(1/2)} C^{k/2}\left(\frac{1}{n-1}\right)^{kH_t}. \tag{3.3}$$

In particular, when $k=2$ one has

$$\mathbb{E}\left(M_t^{(2)}\right) = C\left(\frac{1}{n-1}\right)^{2H_t}, \tag{3.4}$$

with $\text{plim}_{\nu\to\infty} \frac{M_t^{(2)}}{\mathbb{E}\left(M_t^{(2)}\right)} = 1$.

Since C is unknown, one way to get rid of it is first to calculate the quantity

$$M_t'^{(2)} = \frac{2}{\nu}\sum_{i=0}^{\nu/2-1} |X_{t-\frac{2i}{n}} - X_{t-\frac{2(i+1)}{n}}|^2 \tag{3.5}$$

and then observe that

$$\frac{M_t'^{(2)}}{M_t^{(2)}} = \frac{C\left(\frac{2}{n-1}\right)^{2H_t}}{C\left(\frac{1}{n-1}\right)^{2H_t}} = 2^{2H_t}, \tag{3.6}$$

from which one has the estimator

$$\hat{H}_t^{2,\nu,n} = \frac{1}{2}\log_2 \frac{M_t'^{(2)}}{M_t^{(2)}}. \tag{3.7}$$

Since estimator (3.7) is unbiased but with a low rate of convergence, [53] use it to correct the biased estimator of H_t introduced in [54] and refined in [22] which reads as

$$\hat{H}_t^{\nu,n,C^*} = -\frac{\log\left(\frac{1}{\nu}\sum_{i=0}^{\nu-1}|X_{t-\frac{i}{n}} - X_{t-\frac{i+1}{n}}|^2\right)}{2\log(n-1)} + \frac{\log C^*}{\log(n-1)} \tag{3.8}$$

with C^* arbitrarily chosen. The bias is ascribable to the shift dictated by the difference $h = \frac{\log(C^*/C)}{\log(n-1)}$, C being the real unknown parameter of the process. Since the rate of convergence of $\hat{H}_t^{\nu,n,C^*}$ is $\mathcal{O}(\nu^{-1/2}(\log n)^{-1})$, an unbiased estimator with this rate of converge can be built by minimizing the quadratic mean error of the sequence of differences between the two estimates. In fact, denoted by ξ_t a random variable with mean zero, one can write

$$\hat{H}_t^{2,\nu,n} = H_t + \xi_t. \tag{3.9}$$

On the other side, it is also

$$\hat{H}_t^{\nu,n,C^*} = H_t + \frac{\log(C^*/C)}{\log(n-1)}. \tag{3.10}$$

Therefore,

$$h := \frac{\log(C^*/C)}{\log(n-1)} = \hat{H}_t^{\nu,n,C^*} - \hat{H}_t^{2,\nu,n} + \xi_t,$$

from which, by averaging with respect to the number of estimates, it follows

$$h = \frac{1}{n-\nu+1}\sum_{i=\nu}^{n}\left(\hat{H}_t^{\nu,n,C^*} - \hat{H}_t^{2,\nu,n}\right).$$

Since C^* is chosen arbitrarily, the corrected estimate (which does not depend on C) is

$$\hat{H}_t^{(\nu)} = \hat{H}_t^{\nu,n,C^*} - h. \tag{3.11}$$

In [54] it is proved that

$$\hat{H}_t^{\nu,n,C^*}|_{H=0.5} \sim \mathcal{N}\left(0, \frac{1}{2\nu\log^2(n-1)}\right) \tag{3.12}$$

Since the result continues to hold for $\hat{H}_t^{(\nu)}$, this allows to test the significance of the departures of H_t from the equilibrium value 0.5.

Because of (3.1), the quantity $\frac{1}{\nu}\sum_{i=0}^{\nu-1}|X_{t-\frac{i}{n}} - X_{t-\frac{i+1}{n}}|^2$ appearing in the numerator of the first fraction of Eq. (3.8) is an estimate of the variance σ_t^2 of the process increments at time t, for a window of size ν. Thus, denoting it by $\hat{\sigma}_{t,\nu}^2$, one can write

$$\hat{H}_t^{\nu,n,C^*} = -\frac{\log\hat{\sigma}_{t,\nu}^2}{2\log(n-1)} + \frac{\log C^*}{\log(n-1)}$$

that is, setting $w_1 = -\frac{1}{\log(n-1)}$ and $w_2 = \frac{\log C^*}{\log(n-1)}$,

$$\hat{H}_t^{\nu,n,C^*} = w_1\log\hat{\sigma}_{t,\nu} + w_2. \tag{3.13}$$

Eq. (3.13) states the relationship between volatility and regularity, both referred to time t, provided that the Hurst–Hölder exponent is estimated through (3.11). Fig. 1 displays the linear fit (3.13) for the set of S&P500 data that will be analyzed in Section 4. The fit returns an R-square equal to 0.9912, as expected by the analytical nature of the relation. This very relationship shows that the Hurst–Hölder exponent not only retains all the information contained in the volatility, but also expresses when the price process deviates from the martingale condition. Thus, we will investigate the volume–volatility relationship in terms of volume-Hurst/Hölder parameter; this will make it possible to decompose the correlation and study what happens as the degree of market efficiency changes (i.e., as volatility becomes "too high" or "too low" relative to the level that is considered compatible with the equilibrium represented by the semimartingale case).

4. Data and analysis

4.1. Data and preliminary analysis

The analysis considered the daily closing prices and trading volumes of the index S&P500, taken as the benchmark of the U.S. stock market from May, 3rd 1978 to December, 31st 2017 for a sample of 10,005 observations. Following an established practice in the literature, raw trading volumes are converted by natural logarithm and then filtered to

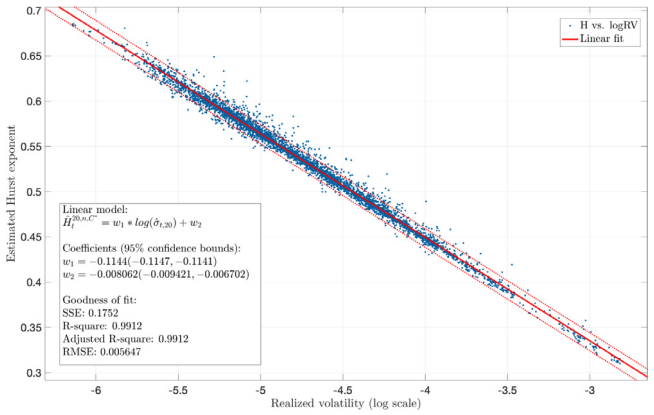

Fig. 1. Relation (3.13) fitted on the series S&P500 analyzed in Section 4. The dotted lines display the 95% confidence bounds. The fit is almost perfect as indicated by the R-square equal to 0.9912.

Table 2
Descriptive statistics and Augmented Dickey–Fuller test. The test specifications are: for R_t and $\tilde{V}_t$, autoregressive model variant (no constant no trend), with critical values: −2.57 (1%), −1.94 (5%), −1.62 (10%). For $\hat{H}_t^{(\nu)}$, autoregressive model with drift variant (constant no trend), with critical values: −3.44 (1%), −2.87 (5%) and −2.57 (10%).

	Mean	Min	Max	StDev	Skewness	Kurtosis	ADF
R_t	0.0003	−0.2290	0.1096	0.0109	−1.1513	30.1988	−102.2726
$\hat{H}_t^{(\nu)}$	0.4995	0.2934	0.6288	0.0454	−0.7221	4.4761	−7.2159
$\tilde{V}_t$	−1.8998	−3.4555	1.5669	0.3884	−0.1022	4.1067	−26.4568

Table 3
Linear fitting models between volume and logarithm of realized volatility, and between volume and the estimated Hurst–Hölder exponent (in parentheses the 95% confidence bounds for the coefficients of the regression).

Fitting model	γ_0	γ_1	SSE	R^2	Adj-R^2	RMSE
(A) $\tilde{V}_t^{(\nu)} = \gamma_0 + \gamma_1 \log \hat{\sigma}_t^{(\nu)}$	2.069 (1.794, 2.345)	0.433 (0.376, 0.490)	38.21	0.318	0.317	0.2845
(B) $\tilde{V}_t^{(\nu)} = \gamma_0 + \gamma_1 \hat{H}_t^{(\nu)}$	2.132 (1.849, 2.415)	−4.267 (−4.832, −3.703)	38.17	0.319	0.317	0.2844

remove the linear trend and avoid spurious regressions, e.g. [55–57]. The descriptive statistics along with the results of the Augmented Dickey–Fuller (ADF) test for stationarity with lag one are reported in Table 2. The assumption of a unit root process is rejected for each series, allowing for a vector-autoregressive analysis. Fig. 2 displays the log-return R_t (top left panel), the corresponding estimates $\hat{H}_t^{(\nu)}$ with $\nu = 21$ (bottom left panel), the log-volumes V_t (top right panel) and the corresponding detrended series ($\tilde{V}_t$) (bottom right panels). The estimates of H_t fluctuate around the value 1/2, and as soon as H_t departs from this value, the market tends to correct its direction and return to equilibrium [58]. Fixing a 95% confidence interval, we deduce that the market can stay far from the equilibrium also for quite long periods and large downward spikes are observed, for example, for October 19, 1987 (Black Monday) or during the financial crisis of 2007–2009, culminating in the collapse of the S&P500 of over 9% on October 15, 2008.

Fig. 3 shows a scatterplot of $\tilde{V}_t$ versus R_t (left panel) and a boxplot of the distribution of R_t for various volume intervals (right panel). The scatterplot reveals that large changes in the index are associated with high volume levels, while the boxplot shows that the dispersion of the distribution of R_t tends to increase with volumes. As expected, these results confirm the existing literature of a positive association between volume and volatility.

4.2. Volume–volatility and efficiency

Before examining the role of (in)efficiency in the correlation between volume and volatility, we observe how the latter is interchangeable with the Hurst exponent estimated through (3.11). This can be seen by the virtually undistinguishable results provided by the two fits between volume and the logarithm of realized volatility, on one side, and between volume and the estimated Hurst–Hölder exponent, on the other (Table 3). All values are estimated ($\hat{H}_t^{(\nu)}$ and $\log \hat{\sigma}_t^{(\nu)}$) or averaged ($\tilde{V}_t^{(\nu)}$) on a window of one trading month ($\nu = 21$). To eliminate the serial dependence which could affect the results of the analysis, we considered data on a monthly time scale.

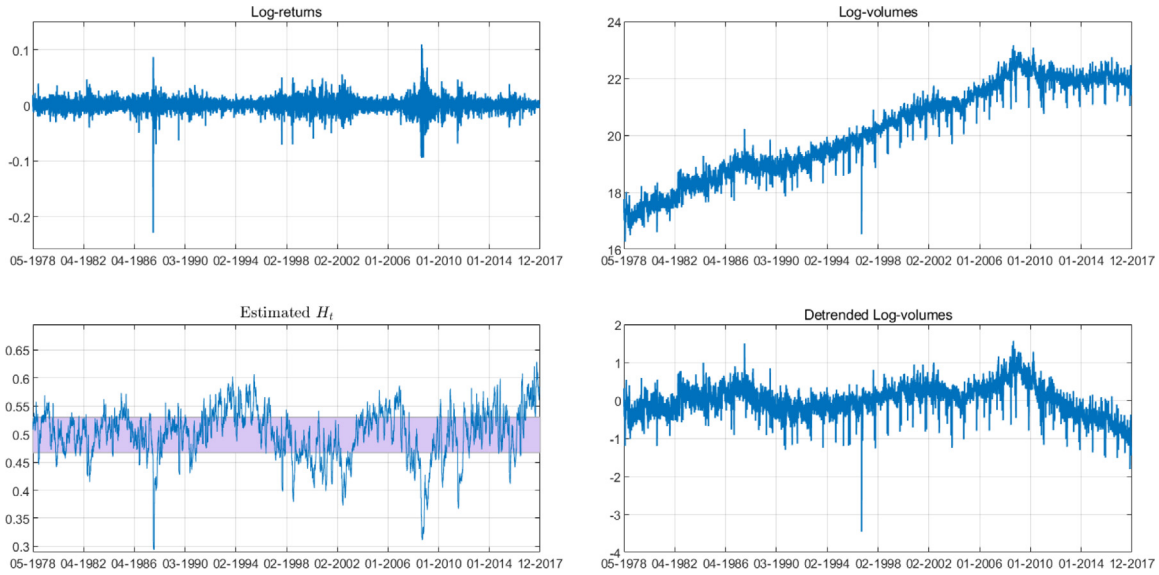

Fig. 2. Top left: log-returns R_t, Top right: log-volumes V_t, Bottom left: estimated Hurst–Hölder exponent $\hat{H}_t^{(\nu)}$ with the confidence interval at $\alpha = 0.05$, Bottom right: detrended log-volumes $\tilde{V}_t$.

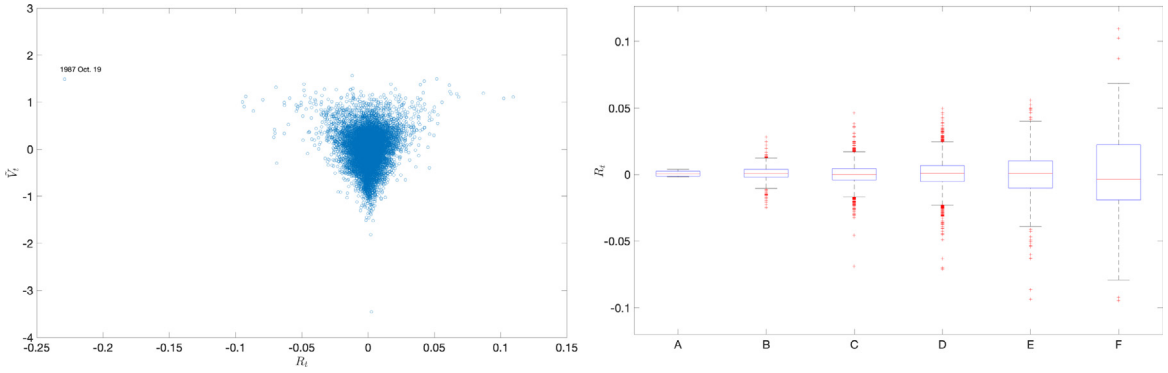

Fig. 3. Dataplots of the contemporaneous price–volume relationship. **Left panel**: scatterplot of $\tilde{V}_t$ against R_t. **Right panel**: boxplots for various volume classes, labeled A through F. The volume classes are in increasing order of standardized log-volume: A, $\tilde{V}_t < -1.4$; B, $-1.4 \le \tilde{V}_t < -0.5$; C, $-0.5 \le \tilde{V}_t < 0$; D, $0 \le \tilde{V}_t < 0.5$; E, $0.5 \le \tilde{V}_t < 1$; F, $1 \le \tilde{V}_t \le 1.6$. The center line in the boxplot is the median of R_t, for each given volume class, the height is the interquartile range, the whiskers represent the 99% interval, and the '+' symbol denotes outliers.

Furthermore, denoted by F the distribution of the log index changes, we define the following subsamples

Negative exceedances	Positive exceedances
$\tilde{V}_t^{(\nu)-} : \tilde{V}_t^{(\nu)} \mapsto \tilde{V}_t^{(\nu)} \mathbb{1}_{\{\tilde{R}_t^{(\nu)} < F^{-1}(\alpha)\}}$	$\tilde{V}_t^{(\nu)+} : \tilde{V}_t^{(\nu)} \mapsto \tilde{V}_t^{(\nu)} \mathbb{1}_{\{\tilde{R}_t^{(\nu)} > F^{-1}(1-\alpha)\}}$
$\hat{H}_t^{(\nu)-} : \hat{H}_t^{(\nu)} \mapsto \hat{H}_t^{(\nu)} \mathbb{1}_{\{\tilde{R}_t^{(\nu)} < F^{-1}(\alpha)\}}$	$\hat{H}_t^{(\nu)+} : \hat{H}_t^{(\nu)} \mapsto \hat{H}_t^{(\nu)} \mathbb{1}_{\{\tilde{R}_t^{(\nu)} > F^{-1}(1-\alpha)\}}$
$\hat{\Sigma}_t^{(\nu)-} : \log \hat{\sigma}_t^{(\nu)} \mapsto \log \hat{\sigma}_t^{(\nu)} \mathbb{1}_{\{\tilde{R}_t^{(\nu)} < F^{-1}(\alpha)\}}$	$\hat{\Sigma}_t^{(\nu)+} : \log \hat{\sigma}_t^{(\nu)} \mapsto \log \hat{\sigma}_t^{(\nu)} \mathbb{1}_{\{\tilde{R}_t^{(\nu)} > F^{-1}(1-\alpha)\}}$

that filter out volumes, Hurst parameters and log-volatilities corresponding to negative or positive exceedances with respect to the quantiles $F^{-1}(\alpha)$ and $F^{-1}(1-\alpha)$, respectively. Fig. 4 displays the correlations for both negative (solid lines) and positive (dotted lines) exceedances, for several critical values of α. In both cases the correlations increase and their behavior is almost identical whether one considers realized volatility or the estimated Hurst–Hölder exponent.

Fig. 5 displays that the correlations with the j-days forward volumes increase for negative exceedances and decrease for positive exceedances, and again the behavior is virtually the same considering volatility or the opposite of the Hurst–Hölder exponent.

To further investigate how volume and Hurst–Hölder exponent co-move and to remove the serial dependence triggered by the window size of the estimator of H_t, as mentioned above, we have sampled the time series at a resolution of ν days;

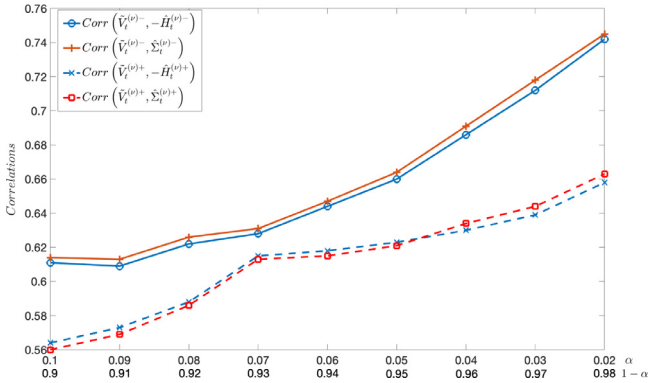

Fig. 4. Correlations for negative (solid lines) and positive (dotted lines) exceedances for different critical values of α. Notice that, because of the inverse relationship (3.13), the positive correlation with the volume is preserved by considering in the formula the opposite of the Hurst–Hölder exponent.

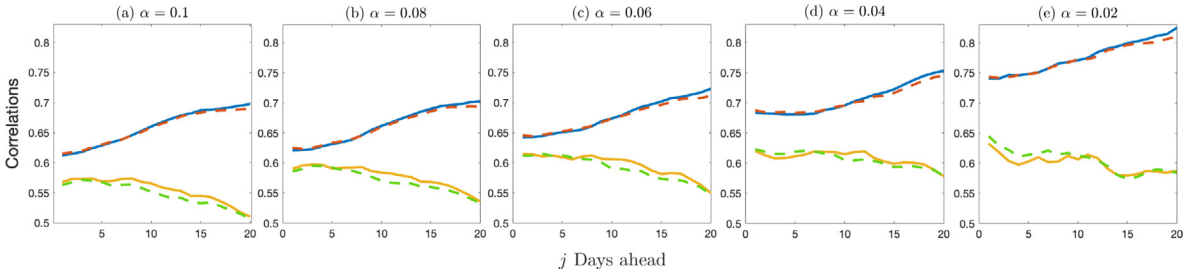

Fig. 5. Blue solid line: $Corr(\tilde{V}^{(\nu)-}_{t+j}, \hat{H}^{(\nu)-}_{t+j})$, Red dotted line: $Corr(\tilde{V}^{(\nu)-}_{t+j}, \hat{\Sigma}^{(\nu)-}_{t+j})$, Yellow solid line: $Corr(\tilde{V}^{(\nu)+}_{t+j}, \hat{H}^{(\nu)+}_{t+j})$, Green dotted line: $Corr(\tilde{V}^{(\nu)+}_{t+j}, \hat{\Sigma}^{(\nu)+}_{t+j})$.

Table 4
Contemporaneous relation, t-statistics in parentheses.

Fitting model (4.1)					Fitting model (4.2)				
α_0	α_1	α_2	F	adj.R^2	β_0	β_1	β_2	F	adj.R^2
0.223*	0.552*	−0.039*	288	0.550	0.356*	0.890*	−0.716*	1740	0.880
[12.552]	[15.558]	[−8.293]			[5.011]	[47.061]	[−5.041]		

*Significant at 1%.

furthermore, the volumes have been averaged over the same previous ν days to align them with the estimates $\hat{H}^{(\nu)}_t$. We have considered the following autoregressive fitting models with respect to both the variables:

$$\hat{H}^{(\nu)}_t = \alpha_0 + \alpha_1 H^{(\nu)}_{t-1} + \alpha_2 \tilde{V}^{(\nu)}_t + e_t \tag{4.1}$$

$$\tilde{V}^{(\nu)}_t = \beta_0 + \beta_1 \tilde{V}^{(\nu)}_{t-1} + \beta_2 \hat{H}^{(\nu)}_t + z_t \tag{4.2}$$

According to MDH, we expect the same sign for coefficients α_1 and β_1, and α_2 and β_2, meaning that both $\tilde{V}^{(\nu)}_t$ and $\hat{H}^{(\nu)}_t$ are driven by the same underlying information flow and, therefore, they change simultaneously.

Table 4 shows that all coefficients are significant and the signs of α_1 and β_1 are both positive, while those of α_2 and β_2 are both negative, as expected. The high values of the F-statistic and of the adjusted R^2 confirm the goodness of fit of the model. The stability of results through time is also confirmed by a monthly rolling-window regression of size equal to the half of the sample (about 20 years). Fig. 6 shows the joint dynamics of α_1 and β_1 (left panel) and α_2 and β_2 (right panel). Both the pairs of values change accordingly, indicating the robustness of the results over time. This is confirmed by the correlation, which is 0.65 between α_1 and β_1, and 0.66 between α_2 and β_2.

From now on, replacing the volatility with the Hurst–Hölder exponent, we exploit the possibility it gives to discriminate periods when the market is efficient from those when it is not. First, we consider the fitting model (B) of Table 3 with respect to the following scenarios:

- **T**: whole sample (Fig. 7, top-left);
- **E**: Efficient market sub-sample, when $\hat{H}^{(\nu)}_t \in \left[\frac{1}{2} - z_{\alpha/2}\sigma, \frac{1}{2} + z_{\alpha/2}\sigma\right]$ (top-right);

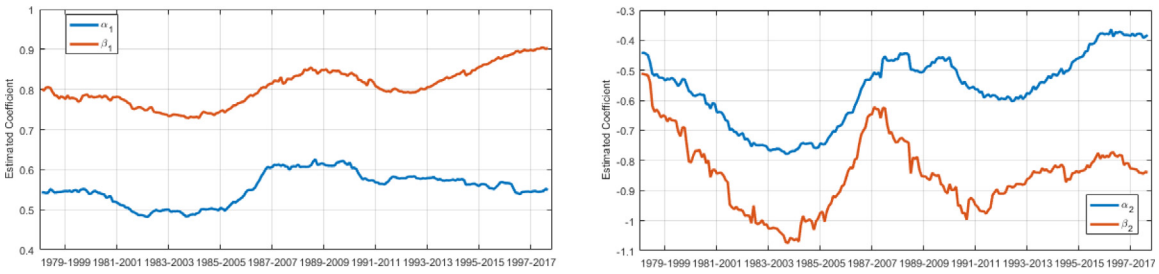

Fig. 6. Dynamic of α_1 and β_1 (left), α_2 and β_2(right). α_2 is multiplied by 10.

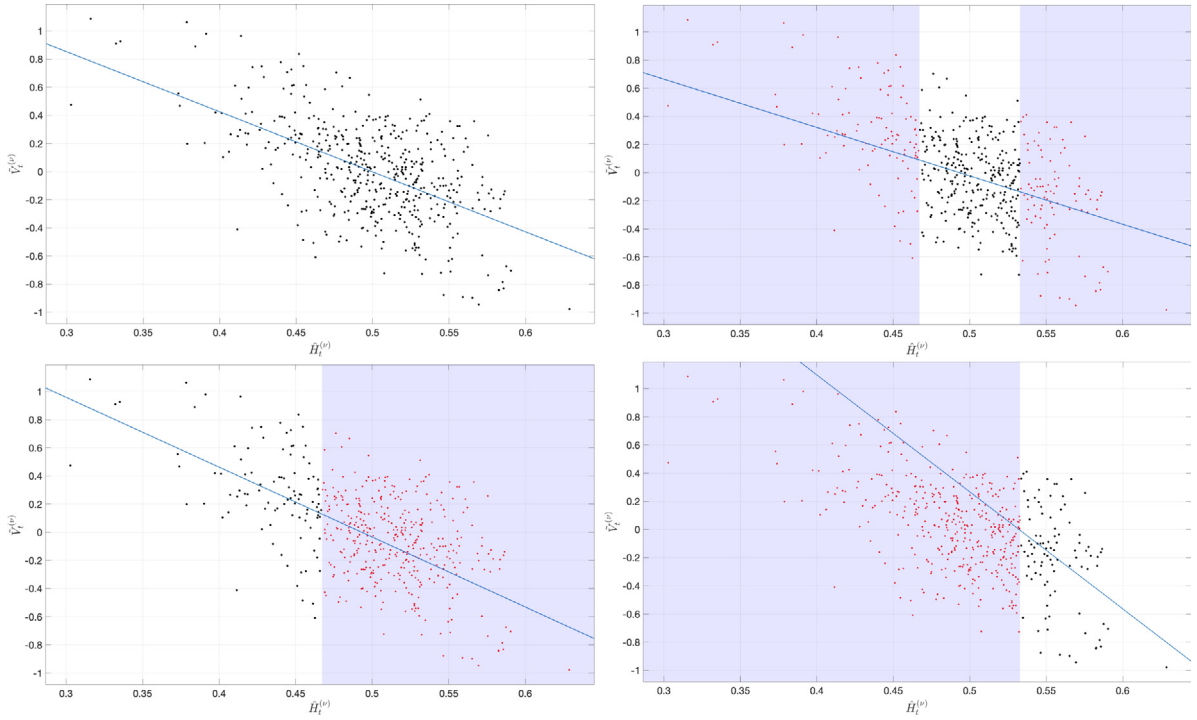

Fig. 7. The volume–volatility relationship adjusted for market efficiency. Top left: scenario **T**; top right: scenario **E**; bottom left: scenario **NI**; bottom right: scenario **PI**.

Table 5
Confidence intervals $U_\alpha = \left[\frac{1}{2} - z_{\alpha/2}\sigma, \frac{1}{2} + z_{\alpha/2}\sigma\right]$ for different values of α.

α:	0.01	0.02	0.03	0.04	0.05
	[0.457, 0.543]	[0.461, 0.539]	[0.464, 0.536]	[0.466, 0.534]	[0.467, 0.533]
α:	0.06	0.07	0.08	0.09	0.10
	[0.469, 0.532]	[0.470, 0.530]	[0.471, 0.530]	[0.472, 0.528]	[0.472, 0.528]

- **NI**: Negative inefficiency sub-sample, when $\hat{H}_t^{(\nu)} \in \left(0, \frac{1}{2} - z_{\alpha/2}\sigma\right)$ (bottom-left);
- **PI**: Positive inefficiency sub-sample, when $\hat{H}_t^{(\nu)} \in \left(\frac{1}{2} + z_{\alpha/2}\sigma, 1\right)$ (bottom-right),

where $z_{\alpha/2}$ is the quantile of the standard normal distribution corresponding to the significance level α and $\sigma = \frac{1}{\sqrt{2\nu}\log(n-1)}$ (see (3.12)). Table 5 summarizes the confidence intervals for different values of α.

Table 6 reports the results for each scenario. For **NI**, **E** and **PI**, the values are relative to the significance level $\alpha = 0.05$, but similar results can be obtained also for $\alpha = 0.10$. Coefficients γ_1 are significant for each scenario, but the R^2 is very close to zero only for scenario **E**, indicating that no relation emerges when the market is efficient. This is confirmed by the Pearson correlation coefficient, which declines towards zero as α increases (columns *Correlation*) only for scenario **E**, while

Table 6
Outputs of regressions. All values of γ are significant at 1% level.

Scenario	γ_0	γ_1	R^2	RMSE	F-stat	Correlation				
						(0.01)	(0.05)	(0.10)	(0.20)	(0.40)
T	2.132	−4.267	0.319	0.284	220.641					
NI	2.450	−4.968	0.226	0.307	28.589	−0.417	−0.475	−0.490	−0.505	−0.512
E	1.713	−3.472	0.059	0.258	17.253	−0.250	−0.245	−0.200	−0.067	−0.000
PI	4.421	−8.308	0.164	0.321	18.236	−0.363	−0.405	−0.336	−0.289	−0.347

Table 7
Contemporaneous relation and efficiency. t-statistics in parentheses.

	λ_0	λ_1	λ_2	λ_3	λ_4	F	adj.R^2
$\alpha = 0.01$	0.259*	0.001	0.482*	−0.070*	0.063*	177	0.602
	[14.852]	[0.439]	[13.883]	[−11.695]	[7.785]		
$\alpha = 0.05$	0.253*	0.002	0.492*	−0.063*	0.059*	171	0.593
	[14.467]	[0.715]	[14.083]	[−11.124]	[7.036]		
$\alpha = 0.10$	0.246*	−0.001	0.507*	−0.058*	0.060*	168	0.589
	[14.168]	[−0.091]	[14.605]	[−10.862]	[6.611]		

*Significant at 1%.

it remains stable for **PI** and increases for **NI**. These findings are also confirmed by the direct observation of those time windows displaying very sharp scenarios; for example, (a) in May 1978–March 1986, the market behaves very efficiently (average Hurst exponent, $\hat{H}_t^{(\nu)} = 0.504$) and in fact the correlation equals 0%, (b) January 2007-June 2009, because of the global financial crisis the market is negatively inefficient ($\hat{H}_t^{(\nu)} = 0.442$), and the correlation equals to $-68,9\%$, (c) March 1992-February 1996, characterized by a rise of price before and during the well- known speculative bubble, the market is positively inefficient ($\hat{H}_t^{(\nu)} = 0.544$), and in fact the correlation equals to $-17,6\%$.

As observed, the degree of dependence between volumes and the Hurst–Hölder parameter is much weaker in efficient periods than in inefficient ones. To analyze with more detail the impact of efficiency, we introduce the dummy variable

$$D_t = \begin{cases} 1, & \text{if } \hat{H}_t^{(\nu)} \in \left[\frac{1}{2} - z_{\alpha/2}\sigma, \frac{1}{2} + z_{\alpha/2}\sigma\right] \\ 0, & \text{otherwise} \end{cases} \tag{4.3}$$

and consider the following regression model:

$$\hat{H}_t^{(\nu)} = \lambda_0 + \lambda_1 D_t + \lambda_2 H_{t-1}^{(\nu)} + \lambda_3 \tilde{V}_t^{(\nu)} + \lambda_4 (\tilde{V}_t^{(\nu)} \cdot D_t) + \varepsilon_t. \tag{4.4}$$

When inefficiency predominates in the market, the volume–volatility correlation is grabbed by λ_3, whereas $\lambda_3 + \lambda_4$ captures the correlation in periods of efficiency. Table 7 displays the results of regression (4.4) for α equals to 0.01, 0.05 and 0.10. As α increases, the confidence interval around 1/2 narrows, indicating greater efficiency; in this case, $\lambda_3 + \lambda_4$ tends to zero, indicating that the volume–volatility correlation vanishes. Fig. 8 shows the values of λ_3 (top panel) and $\lambda_3 + \lambda_4$ (bottom panel) for different values of α and for the three scenarios: **E** (solid black), **NI** (dotted blue) and **PI** (dashed red). Data confirm the results outlined by the correlations in Table 6: as α increases, $\lambda_3 + \lambda_4$ tends to zero, while remaining almost constant when volatility is high (H_t is significantly low, **NI** market) or low (H_t is significantly high, **PI** market). This nonlinear behavior can be

5. Conclusion

The relation between stock price volatility and trading volume has received a remarkable attention over the past decades and constitutes even today a largely debated and controversial issue. In this work, we have investigated whether stock market efficiency can constitute an explanatory variable for the diversity of results achieved during the years. To this end, we have proposed and justified as a measure of market efficiency the Hurst–Hölder dynamic exponent and provided its financial interpretation. Using data for the S&P500 index from 1978 to 2017, we have estimated market efficiency in terms of adherence to the martingale paradigm by means of the Hurst–Hölder exponent H_t. This leads to identify inefficient periods, during which the market displays volatilities which are higher ($H_t < 1/2$) or lower ($H_t > 1/2$) than the value ($H_t = 1/2$) consistent with efficiency. Using the Hurst–Hölder exponent as a measure of volatility, we have found that when efficiency is not accounted for, a positive contemporaneous relationship emerges and is stable over time; conversely, it disappears as soon as efficiency is taken into account. In particular, the positive correlation is pronounced during time frames of high volatility and tends to disappear when market becomes fully efficient. This can explain to some extent the variety of results achieved in literature: a strong/weak positive or even null relation is intimately linked to time-varying degree of efficiency of market and, in its turn, to the capability of market participants to fully discount the information flow.

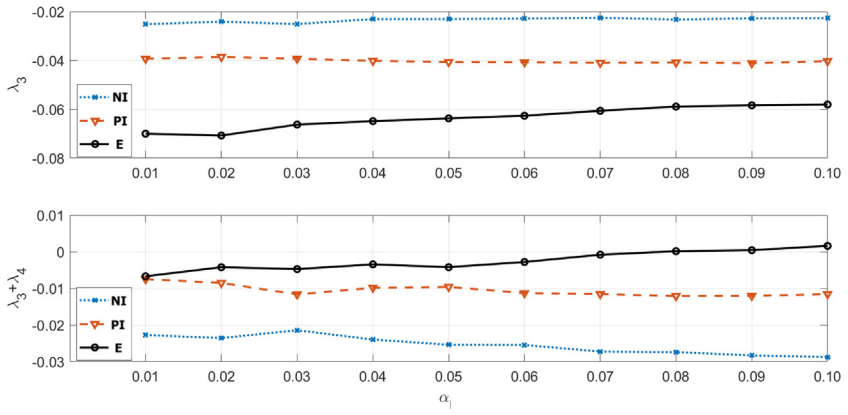

Fig. 8. λ_3 (top panel) and $\lambda_3 + \lambda_4$ (bottom panel) for different values of significance level α.

CRediT authorship contribution statement

Massimiliano Frezza: Data curation, Methodology, Software, Original draft. **Sergio Bianchi:** Conceptualization, Formal analysis, Project administration, Supervision, Writing. **Augusto Pianese:** Formal analysis, Validation, Review & editing.

Declaration of competing interest

The authors declare that they have no known competing financial interests or personal relationships that could have appeared to influence the work reported in this paper.

Data availability

Data will be made available on request.

Acknowledgment

This work was supported by the grant "Progetto di ricerca medio di ateneo 00041-2020" by Sapienza University of Rome.

References

[1] Chen Z, Daigler RT. An examination of the complementary volume-volatility information theories. J Futures Mark 2008;28(10):963–92.
[2] Clark PK. A subordinated stochastic process model with finite variance for speculative prices. Econometrica 1973;41:135–56.
[3] Epps TW, Epps ML. The stochastic dependence of security price changes and transaction volumes: Implications for the mixture-of-distributions hypothesis. Econometrica 1976;44(2):305–21.
[4] Rogalski RJ. The dependence of prices and volume. Rev Econ Stat 1978;60(2):268–74.
[5] Tauchen G, Pitts M. The price variability-volume relationship on speculative markets. Econometrica 1983;51(2):485–505.
[6] Harris L. Cross-security tests of the mixture of distributions hypothesis. J Financ Quant Anal 1986;21(01):39–46.
[7] Kawaller IG, Koch PD, Koch TW. Intraday relationships between volatility in S&P500 futures prices and volatility in the S&P500 index. J Bank Financ 1990;14(2):373–97.
[8] Andersen TG. Return volatility and trading volume: An information flow interpretation of stochastic volatility. J Finance 1996;51(1):169–204.
[9] Copeland TE. A model of asset trading under the assumption of sequential information arrival. J Finance 1976;31(4):1149–68.
[10] Morse D. Price and trading volume reaction surrounding earnings announcements: a closer examination. J Account Res 1981;19:374–83.
[11] Jennings RH, Starks LT, Fellingham JC. An equilibrium model of asset trading with sequential information arrival. J Finance 1981;36:143–61.
[12] Jennings RH, Barry CB. Information dissemination and portfolio choice. J Financ Quant Anal 1983;18:1–19.
[13] Bessembinder H, Seguin P. Price volatility, trading volume, and market depth: Evidence from futures markets. J Financ Quant Anal 1993;28(1):21–39.
[14] Varian HR. Divergence of opinion in complete markets. J Finance 1985;40:309–17.
[15] Varian HR. Differences of opinion in financial markets. In: (Ed.) CS, Financial Risk: Theory E, Implications, editors. Proceedings of the eleventh annual economic policy conference of the federal reserve bank of St. Louis. Boston: Kluwer; 1989, p. 3–37.
[16] Shalen CT. Volume, volatility, and the dispersion of beliefs. Rev Financ Stud 1993;6(2):405–34.
[17] Harris M, Raviv A. Differences of opinion make a horse race. Rev Financ Stud 1993;6:473–506.
[18] DeLong JB, Shleifer A, Summers LH, Waldmann RJ. Noise trader risk in financial markets. J Polit Econ 1990a;98:703–38.
[19] DeLong JB, Shleifer A, Summers LH, Waldmann RJ. Positive feedback investment strategies and destabalized rational speculation. J Finance 1990b;45:379–95.
[20] Cajueiro DO, Tabak BM. The hurst exponent over time: testing the assertion that emerging markets are becoming more efficient. Physica A 2004;336(3–4):521–37.

[21] Eom C, Choi S, Oh G, Jung W-S. Hurst exponent and prediction based on weak-form efficient market hypothesis of stock markets. Physica A 2008;387(18):4630–6.
[22] Bianchi S, Pantanella A, Pianese A. Modeling stock prices by multifractional Brownian motion: an improved estimation of the pointwise regularity. Quant Finance 2013;13(8):1317–30.
[23] Horta P, Lagoa S, Martins L. The impact of 2008 and 2010 financial crises on the hurst exponents of international stock markets: implications for efficiency and contagion. Int Rev Financ Anal 2014;35:140–53.
[24] Garcin M. Estimation of time-dependent hurst exponents with variational smoothing and application to forecasting foreign exchange rates. Physica A 2017;483(Supplement C):462–79.
[25] Bianchi S, Frezza M. Fractal stock markets: International evidence of dynamical (in)efficiency. Chaos 2017;27(7):071102.
[26] Risso WA. The informational efficiency and the financial crashes. Res Int Bus Finance 2008;22(3):396–408.
[27] Brouty X, Garcin M. A statistical test of market efficiency based on information theory. 2022, preprint. Papers 2208.11976, arXiv.org.
[28] Ito M, Noda A, Wada T. International stock market efficiency: a non-Bayesian time-varying model approach. Appl Econ 2014;46(23):2744–54.
[29] Ammy-Driss A, Garcin M. Efficiency of the financial markets during the COVID-19 crisis: Time-varying parameters of fractional stable dynamics. Physica A 2023;609:128335.
[30] Feng W, Yang Y, Yuan Q, Gu C, Yang H. Evolution of scaling behaviors in currency exchange rate series. Fractals 2019;27:1950005.
[31] Kristoufek L, Vosvrda M. Measuring capital market efficiency: Global and local correlations structure. Physica A 2013;392(1):184–93.
[32] Fama EF. Efficient capital markets: A review of theory and empirical work. J Finance 1970;25(2):383–417.
[33] Bianchi S, Pianese A. Multifractional properties of stock indices decomposed by filtering their pointwise hölder regularity. Int J Theor Appl Financ 2008;11(6):567–95.
[34] Mandelbrot BB, Van Ness JW. Fractional Brownian motions, fractional noises and applications. SIAM Rev 1968;10(4):422–37.
[35] Rogers LCG. Arbitrage with fractional Brownian motion. Math Finance 1997;7(1):95–105.
[36] Hu Y, Nualart D, Song J. Fractional martingales and characterization of the fractional Brownian motion. Ann Probab 2009;37(6):2404–30.
[37] Péltier RS, Lévy Véhel J. Multifractional Brownian motion: Definition and preliminary results. Rapport de recherche inria 2645, Programme 4 (robotique, image et vision - action fractales), 1-39, 1995, p. 1–39.
[38] Ayache A, Lévy Véhel J. On the identification of the pointwise Höder exponent of the generalized multifractional brownian motion. Stoch Process Appl 2004;111(1):119–56.
[39] Lim SC, Eab CH. Some fractional and multifractional Gaussian processes: A brief introduction. Int J Mod Phys: Conf Ser 2015;36:1560001.
[40] Loboda D, Mies F, Steland A. Regularity of multifractional moving average processes with random Hurst exponent. Stochastic Process Appl 140.
[41] Ayache A, Bouly F. Moving average multifractional processes with random exponent: Lower bounds for local oscillations. Stochastic Process Appl 146.
[42] Benassi A, Jaffard S, Roux D. Gaussian processes and pseudodifferential elliptic operators. Rev Math Iberoam 1997;13:19–89.
[43] Benassi A, Cohen S, Istas J. Identifying the multifractional function of a Gaussian process. Statist Probab Lett 1998;39:337–45.
[44] Falconer KJ. Tangent fields and the local structure of random fields. J Theoret Probab 2002;15(3):731–50.
[45] Coeurjolly JF. Identification of multifractional Brownian motion. Bernoulli 2005;11(6):987–1008.
[46] Bianchi S, Pantanella A, Pianese A. Efficient markets and behavioral finance: a comprehensive multifractional model. Adv Complex Syst 2015;18(1–2):1550001:1–29.
[47] Luo J, Subrahmanyam A, Titman S. Momentum and reversals. When overconfident investors underestimate their competition. Rev Financ Stud 2021;34(1):351–93.
[48] Istas J, Lang G. Variations quadratiques et estimation de l'exposant de hölder local d'un processus gaussien. Ann Inst H. Poincaré 1997;33(4):407–36.
[49] Kent JT, Wood ATA. Estimating the fractal dimension of a locally selfsimilar Gaussian process using increments. J R Stat Soc Ser B 1997;59(3):679–700.
[50] Benassi A, Bertrand P, Cohen S, Istas J. Identification of the hurst index of a step fractional Brownian motion. Stat Inference Stoch Process 2000;3(1–2):101–11.
[51] Coeurjolly JF. Estimating the parameters of a fractional Brownian motion by discrete variations of its sample paths. Stat Inference Stoch Process 2001;4(2):199–227.
[52] Péltier RS, Lévy Véhel J. A new method for estimating the parameter of fractional Brownian motion. Rapport de recherche INRIA 2396, Programme 4 (robotique, image et vision - action fractales), 1994, p. 1–27.
[53] Pianese A, Bianchi S, Palazzo AM. Fast and unbiased estimator of the time-dependent hurst exponent. Chaos 2018;28(31102):1–6.
[54] Bianchi S. Pathwise identification of the memory function of the multifractional Brownian motion with application to finance. Int J Theor Appl Finance 2005;8(2):255–81.
[55] Gallant A, Rossi P, Tauchen G. Stock prices and volume. Rev Financ Stud 1992;5(2):199–242.
[56] Park B-J. Surprising information, the MDH, and the relationship between volatility and trading volume. J Financial Mark 2010;13(3):344–66.
[57] Koubaa Y, Skander S. The relationship between trading activity and stock market volatility: Does the volume threshold matter? Econ Model 2019;82:168–84.
[58] Frezza M. Modeling the time-changing dependence in stock markets. Chaos Solitons Fractals 2012;45:1510–20.